Article

Not peer-reviewed version

C14DM Ablation Leads to Reduced Tolerance to Plasma Membrane Stress and Increased Drug Sensitivity in *Leishmania major*

Samrat Moitra , Sumit Mukherjee , Veronica L Hernandez , Kai Zhang *

Posted Date: 4 August 2025

doi: 10.20944/preprints202508.0200.v1

Keywords: *Leishmania*; Sterol; Synergy

 doi:10.20944/preprints202508.0200.v1

Article

C14DM Ablation Leads to Reduced Tolerance to Plasma Membrane Stress and Increased Drug Sensitivity in *Leishmania major*

Samrat Moitra [1], Sumit Mukherjee [1,2], Veronica Hernandez [1] and Kai Zhang [1,*]

[1] Department of Biological Sciences, Texas Tech University, Lubbock, TX 79409, USA

[2] Current address: Department of Biology, Texas State University, San Marcos, TX 78666, USA

* Correspondence: kai.zhang@ttu.edu; Tel.: 1-806-834-0550

Abstract

Sterol biosynthesis is crucial for the function of biological membranes and an important target for anti-protozoan/anti-fungal drugs. In the trypanosomatid parasite *Leishmania major*, deletion of sterol C14-demethylase (C14DM) results in hypersensitivity to heat, increased plasma membrane fluidity, profound mitochondrial dysfunctions, and reduced virulence in mice. In this study, we show that C14DM-null mutants are defective in their tolerance to membrane disrupting agents and osmotic stress and their ability to form autophagosomes. In addition, C14DM-null mutants exhibit heightened sensitivity to anti-trypanosomatid drugs including antimony, ethidium bromide and pentamidine. Combination of itraconazole (a C14DM antagonist) and pentamidine synergistically inhibit the growth of *Leishmania* parasites. These findings reveal new insight into the roles of sterol synthesis in protozoan pathogens and highlight the potential of using drug combinations to achieve better treatment outcome.

Keywords: *Leishmani*a; Sterol; Synergy

1. Introduction

Trypanosomatid parasites of the genus *Leishmania* cause a spectrum of diseases from localized skins lesions to potentially lethal infections of the liver, spleen and bone marrow. During their life cycle, these protozoans transition between flagellated promastigotes in sandflies and non-flagellated amastigotes in macrophages. To survive in the vector and mammalian hosts, *Leishmania* parasites must withstand challenges from digestive enzymes, plasma membrane stress, nutrient restriction, and adaptive immunity [1]. Understanding the mechanisms by which *Leishmania* utilizes to counter various stress may lead to the development of better treatments. This is significant because current drugs are plagued with high toxicity, low efficacy and resistance is on the rise [2].

Sterols are essential components of the plasma membrane regulating membrane fluidity and permeability. Inhibitors of sterol biosynthesis have been explored as drugs against fungi and trypanosomatids [3–5]. Among the 20 or so enzymes involved in sterol synthesis, a prominent drug target is the cytochrome P450-dependent sterol 14α-demethylase (C14DM). In *Leishmania major*, genetic or chemical ablation of C14DM leads to accumulation of 14-methylated sterol intermediates and loss of ergostane-based sterols; the C14DM-null mutants (*c14dm*$^-$) show increased plasma membrane fluidity, hindered mitochondrial respiration, reduced translation efficiency, and hypersensitivity to heat and glucose restriction; yet despite these defects, *c14dm*$^-$ mutants are viable as promastigotes in culture and as amastigotes in mice although with slower growth rates [6–8]. In *Leishmania donovani*, an early study using the plasmid complementation method failed to generate the chromosomal C14DM-null mutant [9], yet a later report using the CRISPR-Cas9 based gene deletion approach successfully produced the mutant [10], questioning the essentiality of C14DM in *L. donovani*. These and other findings suggest that the inhibition of C14DM alone may not be sufficient

 doi:10.20944/preprints202508.0200.v1

to clear *Leishmania* infection [11–13]. Meanwhile, the anti-*Leishmania* effects of C14DM inhibitors such as azoles may be enhanced if they are used in combination with other chemicals including those targeting the weaknesses displayed by *c14dm*$^-$ [7,14,15].

In this study, we evaluated the sensitivity of *L. major c14dm*$^-$ mutants to plasma membrane disrupting agents and explored the potential of using inhibitor combinations against several *Leishmania* parasite species. Results showed that the fitness costs of C14DM inhibition could be exploited for better anti-*Leishmania* therapy.

2. Results

2.1. C14dm$^-$ *Mutants Are Hypersensitive to Triton X-100, Dimethyl Sulfoxide (DMSO), and Osmotic Changes*

In L. major, C14DM inactivation leads to increased plasma membrane fluidity and failure to retain vital components of lipid rafts such as GP63 [6]. To further explore how changes in sterol composition affect membrane stability, log phase promastigotes were incubated in complete M199 media containing 0.0125% Triton X-100. Cell survival was monitored by the propidium iodide exclusion assay. As a non-ionic detergent, Triton X-100 can generate small pores in the membrane at low concentrations [16]. After 1- and 3-hours incubation, about 50% and 90% of c14dm$^-$ mutants became permeable to propidium iodide (indicating cell death) respectively, in comparison to <30% for L. major wild type (WT) and the complemented c14dm$^-$/+C14DM parasites after 6 hours of incubation in the same condition (Figure 1A). Similar results were observed when log phase promastigotes were challenged with 0.9% DMSO, another membrane permeabilization agent, for a period of 1–4 hours (Figure 1B). Thus, C14DM inactivation causes hypersensitivity to membrane disrupting chemicals.

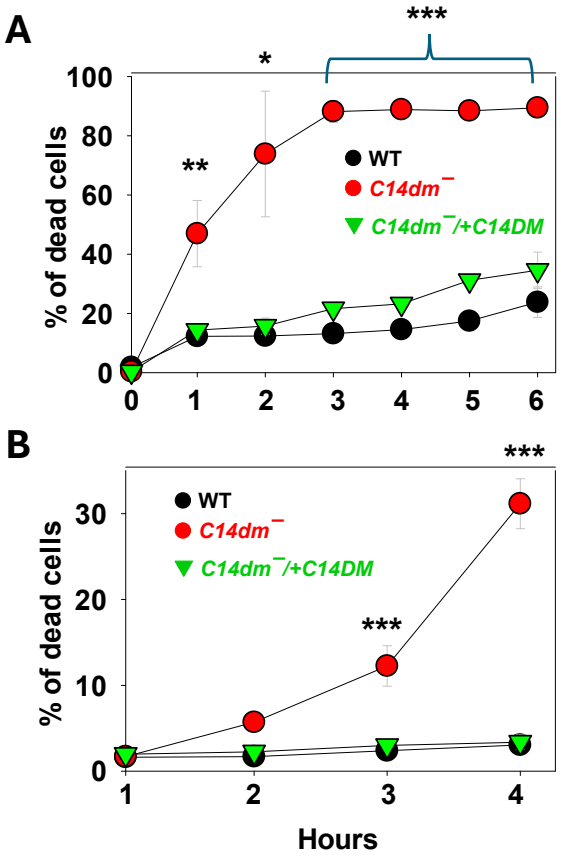

Figure 1. C14dm$^-$mutants are hypersensitive to membrane perturbation agents. Log phase promastigotes of WT, c14dm$^-$, and c14dm$^-$/+C14DM were treated with 0.0125% of Triton X-100 (**A**) or 0.9% of DMSO (**B**).

 doi:10.20944/preprints202508.0200.v1

Percentages of dead cells were determined hourly by flow cytometry after propidium iodide staining. Error bars represent standard deviations from three repeats.

Along the same lines, we examined whether C14DM plays a role in osmoregulation. L. major WT, c14dm$^-$ and c14dm$^-$/+C14DM promastigotes were cultivated in their regular media (complete 1 x M199) [17], and then subjected to isotonic (Figure 2A), hypotonic (0.5 x, Figure 2B) or hypertonic (2.5 x, Figure 2C) conditions. Their cell volume change was measured by light-scattering spectrophotometry as previously described [18]. This method monitors the swelling, shrinking and recovery of cells in response to osmotic changes. Under hypotonic stress, c14dm$^-$ mutants showed more severe swelling than WT and c14dm$^-$/+C14DM parasites after 2–3 min as indicated by reduced light absorbance. After 15–20 min, c14dm$^-$ mutants recovered to similar levels as WT and c14dm$^-$/+C14DM (Figure 2B). With hypertonic challenge, c14dm$^-$ mutants shrank more than WT and c14dm$^-$/+C14DM cells (Figure 2C) and were unable to restore their volume to the same degree during the period of the experiment (up to 60 min). Therefore, c14dm$^-$ mutants are hypersensitive to osmotic stress.

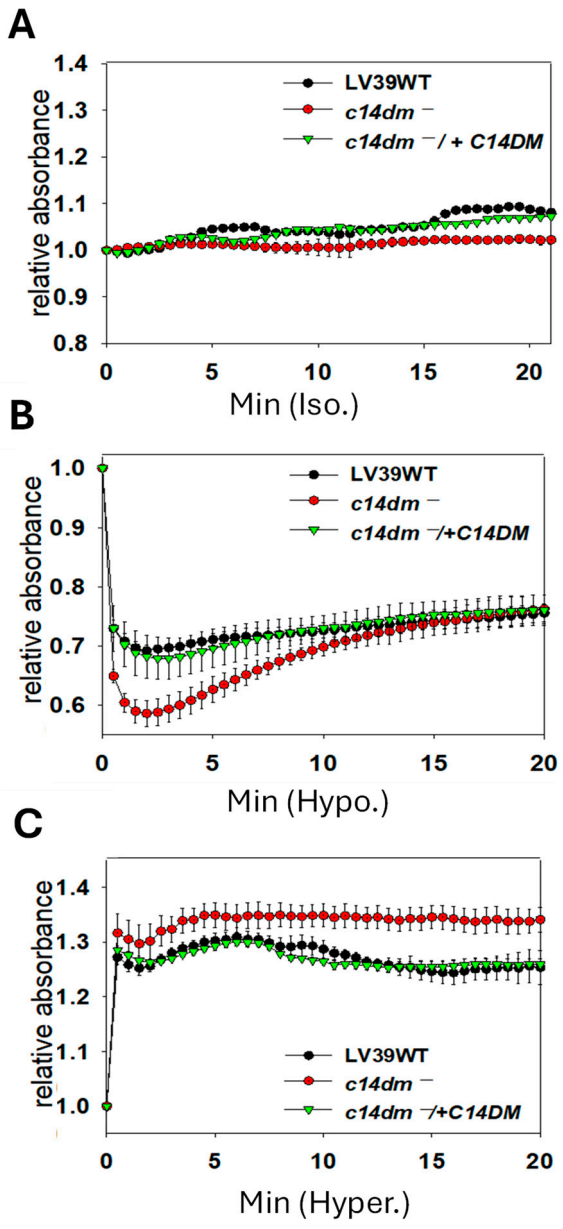

Figure 2. C14dm$^-$mutants show altered response to osmotic stress. Log phase promastigotes were resuspended in isotonic (**A**, 300 mOsmol/L), hypotonic (**B**, 150 mOsmol/L), or hypertonic (**C**, 600 mOsmol/L) solution as

 doi:10.20944/preprints202508.0200.v1

described in Materials and Methods. Response to osmotic changes (regulatory volume decrease/increase) were monitored by light scattering measurements at 550 nm using a Biotek plate reader (every 30 sec for 60 min). Error bars represent standard deviations from four repeats.

2.2. C14dm⁻ Mutants Show Hypersensitivity to Pseudomonas aeruginosa Spent Medium and Pyocyanin

Leishmania protozoans are vector-borne parasites which form complex interactions with bacteria both in the sandfly and the mammalian host's skin. Various bacterial species may affect Leishmania development and disease progression through competition for nutrients, production of toxins, and modulation of the host's immune response [19–22]. Here we examined the response of L. major promastigotes to the metabolites of Pseudomonas aeruginosa, a gram-negative opportunistic bacterium that has been identified from multiple sandfly species [23]. To do so, P. aeruginosa strain PA14 was cultivated in complete 1 x M199 medium (the same medium for growing Leishmania promastigotes) until the OD600 reached 3.0; the spent medium was isolated by centrifugation and filtration; and log phase parasites were incubated in the PA14 spent medium and their survival was monitored by direct cells counting. As summarized in Figure 3A, the PA14 spent medium is highly toxic to L. major promastigotes. For WT and c14dm⁻/+C14DM, ~20% of the parasites remained viable after 90 min. In comparison, c14dm⁻ mutants were even more sensitive: after 10 min, only ~10% were viable and after 60 min, all of them were lysed. The potent leishmanicidal activity of PA14 spent medium is likely due to the plethora of cytolytic toxins produced by P. aeruginosa [24,25].

We also explored whether C14DM is involved in tolerance to other cytotoxic products from P. aeruginosa such as pyocyanin, a water-soluble, phenazine-derived pigment metabolite capable of inducing reactive oxygen species (ROS) in target cells [26,27]. When grown in the presence of pyocyanin (0–250 µM), c14dm⁻ mutants showed a significant and dose dependent level of cell death (33–70%) after 24 hours. WT and add-back parasites were not affected by the pyocyanin treatment at the same concentration range (Figure 3B). Together, these findings demonstrate the importance of sterol synthesis in Leishmania resistance to P. aeruginosa products.

 doi:10.20944/preprints202508.0200.v1

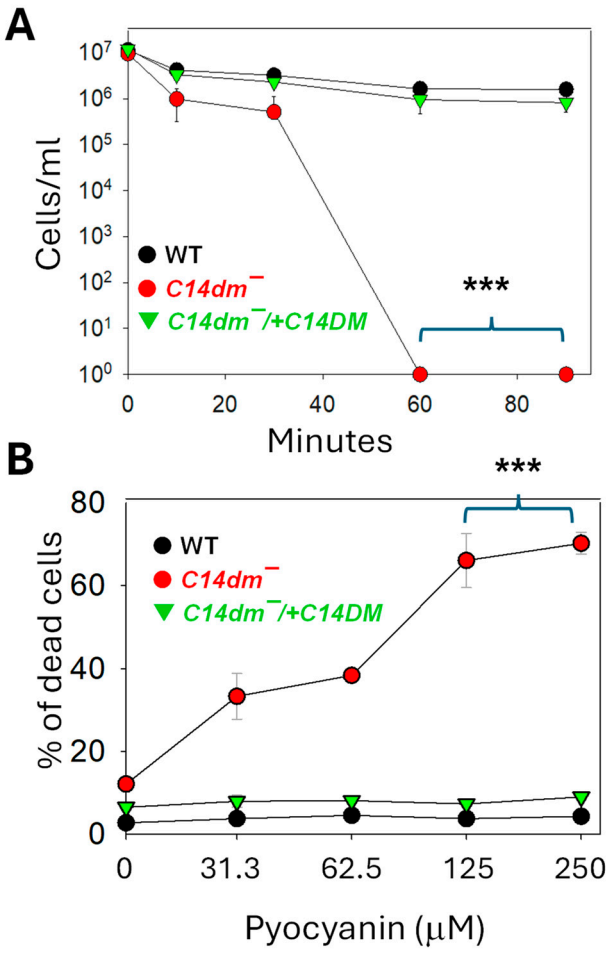

Figure 3. C14dm⁻mutants are hypersensitive to Pseudomonas aeruginosa products. Log phase promastigotes of WT, c14dm⁻, and c14dm⁻/+C14DM were incubated in Pseudomonas aeruginosa PA14 spent medium (**A**) or various concentrations of pyocyanin (**B**) as described in Materials and Methods. In **A**, the remaining cells/ml were monitored at 0–90 minutes post incubation. In **B**, percentages of dead cells were determined hourly by flow cytometry after 24 hours. Error bars represent standard deviations from four repeats.

2.3. C14dm⁻ Mutants Show Autophagy Defects

Consistent with their mitochondrial deficiencies, the c14dm⁻ mutants are more dependent on glucose uptake and glycolysis than WT parasites for energy production [7]. Consequently, they are extremely vulnerable to glucose starvation. Here we investigate whether the capacity to carry out autophagy may also contribute to the compromised response of c14dm⁻ mutants to starvation by introducing GFP-ATG8 (a known marker for macroautophagy) into promastigotes and then monitoring its cellular location and lipidation [28,29]. As WT promastigotes grew in culture, GFP-ATG8 transitioned from mostly cytoplasmic in log phase to 40–80% punctate structures in stationary phase, indicating increased formation of autophagosomes as parasites encountered reduced nutrient levels in culture (Figure 4A–C and supplemental Figures S1 and S2) [28,29]. In c14dm⁻, GFP-ATG8 displayed an uneven, tubular, intracellular distribution during log phase and only 8–36% of cells showed GFP-ATG8 puncta in stationary phase (Figure 4A–C and supplemental Figures S1 and S2). These anomalies were largely reversed to WT-levels in the c14dm⁻/+C14DM add-back parasites. We also examined the lipidation of GFP-ATG8 by Western blot. While log phase parasites mainly contained the non-lipidated GFP-ATG8, stationary phase parasites had both non-lipidated and fast migrating lipidated GFP-ATG8 (GFP-ATG8-PE). Compared to WT cells, c14dm⁻ mutants had less GFP-ATG8-PE during the stationary phase (Figure 4D,E and supplemental Figures S1 and S2). The formation of GFP-ATG8 puncta and the lipidation of GFP-ATG8 are considered autophagy markers

 doi:10.20944/preprints202508.0200.v1

in Leishmania promastigotes under starvation conditions or during differentiation [28–30]. Thus, our findings suggest that c14dm⁻ mutants are deficient in autophagy.

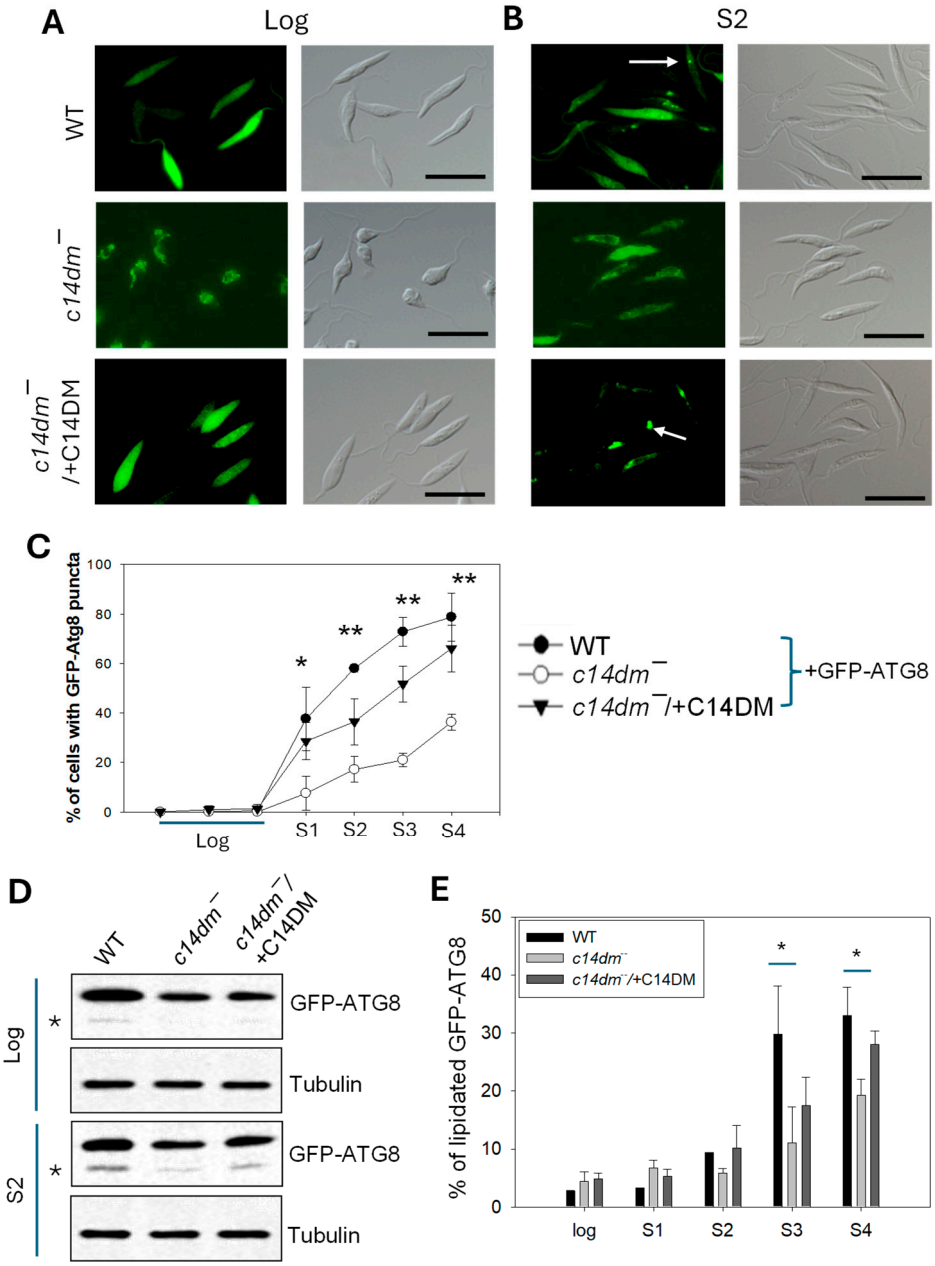

Figure 4. C14dm⁻ mutants show defects in autophagy. Promastigotes of WT, c14dm⁻, and c14dm⁻/+C14DM containing GFP-ATG8 were cultivated from log phase to stationary phase (day 1-day 4 as S1-S4). (**A**-**C**) The formation of GFP-ATG8 puncta representing autophagosomes (examples were marked by arrows) was monitored by fluorescence microscopy. Representative fluorescence images and DIC images were shown in **A** (log) and **B** (S2). Quantified results were shown in **C**. Scale bars in **A**-**B**: 10 µm. (**D**-**E**) Lipidation of GFP-ATG8 was determined by Western blot using an anti-GFP antibody (in **D**, asterisks represent lipidated GFP-ATG8). The anti-tubulin antibody was used as a loading control. (**E**) Quantitation of Western blots showing the percentages of lipidated GFP-ATG8. Error bars represent standard deviations from three repeats. More microscopy and Western blot images are included in supplemental Figures S1 and S2.

2.4. C14dm⁻ Parasites Show Increased Sensitivity to Antimony and Ethidium Bromide (EtBr)

The hypersensitivity of c14dm⁻ mutants to various stress conditions including heat, starvation, membrane perturbation and osmolality change prompts us to investigate whether such

 doi:10.20944/preprints202508.0200.v1

hypersensitivity can be exploited to develop better antileishmanial agents. We first tested the efficacy of potassium antimony (III) tartrate, a classic drug used to treat leishmaniasis and trypanosomiasis [2,31]. In culture, c14dm⁻ mutants showed a dose-dependent response with an EC50 of 6.3 ± 0.6 µM, which was significantly lower than WT (EC50: 19.0 ± 1.3 µM) and c14dm⁻/+C14DM promastigotes (EC50: 39.2 ± 3.0 µM). Similarly, c14dm⁻ mutants were much more sensitive to EtBr which interferes with kDNA replication and causes growth arrests [32,33] than WT and add-back L. major promastigotes (Figure 5B; EC50 for c14dm⁻: 32 ± 2.4 nM; EC50 for WT and c14dm⁻/+C14DM: 250–280 nM).

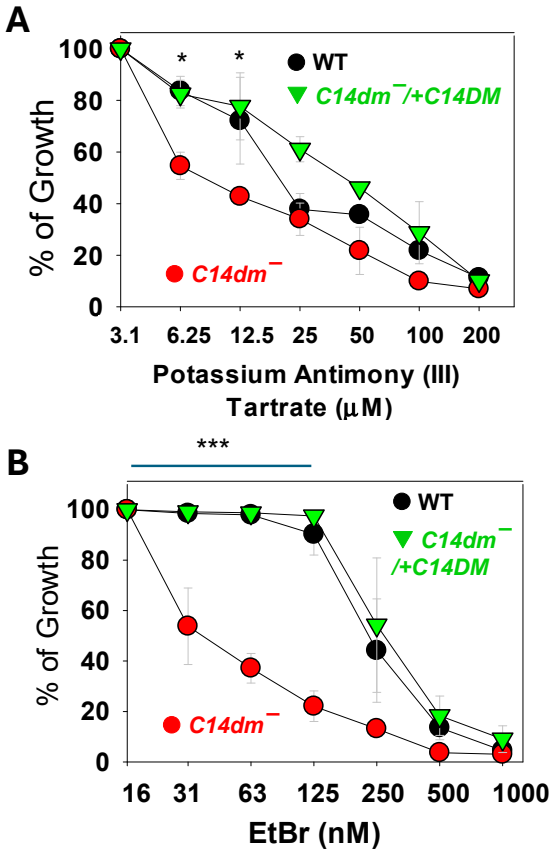

Figure 5. C14dm⁻ mutants are hypersensitive to antimony III and ethidium bromide (EtBr). Log phase promastigotes of WT, c14dm⁻, and c14dm⁻/+C14DM were cultivated in the presence of potassium antimony (III) tartrate (**A**) or EtBr (**B**). Cell growth was monitored after 48 hours and compared to cultures grown in the absence of drugs. Error bars represent standard deviations from three repeats.

2.5. Synergistic Inhibition of Leishmania mexicana and Leishmania donovani with Pentamidine (PENT) and Itraconazole (ITZ)

In L. major, genetic or chemical ablation of C14DM causes increased susceptibility to PENT, an anti-trypanosomatids agent known to be sequestered in the mitochondria of target cells [7,34]. Here we tested whether this finding could be extended to other Leishmania species.

For Leishmania donovani and Leishmania mexicana promastigotes, their EC50s to PENT were 1.01 ± 0.039 µM and 1.28 ± 0.099 µM, respectively (Figure 6). To generate c14dm⁻ phenocopies, we cultivated cells in the presence of ITZ, a C14DM inhibitor [6]. The EC50s to ITZ for L. donovani and L. mexicana were 0.84 ± 0.24 µM and 0.64 ± 0.178 µM, respectively (Figure 6). When grown in low concentrations of ITZ (<EC50 values), the sensitivities of L. donovani and L. mexicana to PENT were determined and their EC50 values for PENT were plotted in an isobologram (Figure 6). Both L. donovani and L. mexicana were more susceptible to PENT in the presence of low dose ITZ, indicating

 doi:10.20944/preprints202508.0200.v1

that PENT and ITZ work synergistically [35]. The mean fractional inhibitory concentration (FIC) for PENT and ITZ was determined to be 0.29 ± 0.054 for L. donovani and 0.33 ± 0.087 for L. mexicana (FIC<0.5 is considered synergistic) [35].

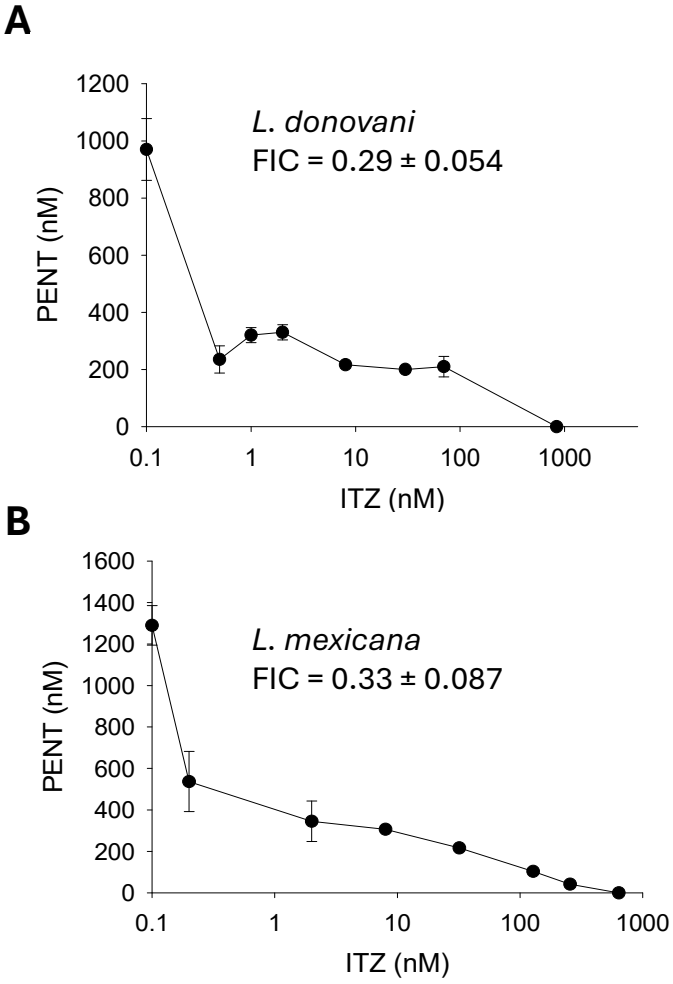

Figure 6. Synergistic inhibition of Leishmania promastigotes with itraconazole (ITZ) and pentamidine (PENT). Log phase promastigotes of L. donovani (**A**) or L. mexicana (**B**) were cultivated in various concentrations of ITZ (X axis) and PENT (Y axis). EC50 values were determined and plotted in an isobologram. Fractional inhibitory concentrations (FIC) were calculated as described in **Materials and Methods** (average ± SDs). Error bars represent standard deviations from four repeats.

2.6. C14DM Inhibition Enhances Drug Sensitivity in L. mexicana axenic Amastigotes

Finally, we examined the impact of C14DM inhibition on the drug susceptibility of L. mexicana axenic amastigotes which mimic intracellular amastigotes [36]. When cultivated in the presence of 50 nM of ITZ, axenic amastigotes of L. mexicana displayed heightened sensitivity to potassium antimony III tartrate (EC50: 98 ± 10 nM) and PENT (EC50: 1.0 ± 0.06 μM); both values are significantly lower than those without ITZ (EC50 for antimony III without ITZ: 8.3 ± 0.44 μM; EC50 for PENT without ITZ: >12 μM); thus, C14DM inhibition by ITZ may enhance drug sensitivity in Leishmania amastigotes (Figure 7).

 doi:10.20944/preprints202508.0200.v1

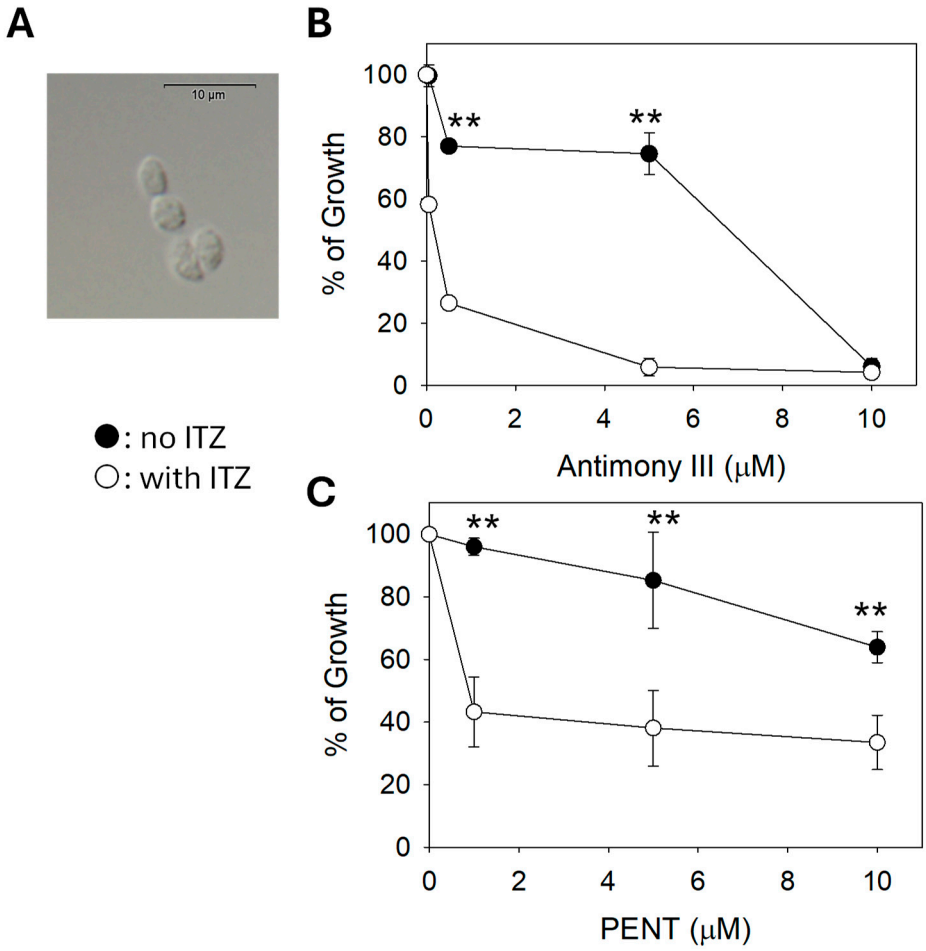

Figure 7. Chemical inhibition of C14DM makes L. mexicana axenic amastigotes hypersensitive to antimony III and pentamidine (PENT). Axenic amastigotes of L. mexicana (A) cultivated in the absence or presence of 50 nM of ITZ were treated with various concentrations of potassium antimony III tartrate (B) or PENT (C). Cell growth was monitored after 72 hours in comparison to cells growing in the absence of ITZ. Error bars represent standard deviations from four repeats.

3. Discussion

C14DM catalyzes the heme-dependent oxidative removal of the C-14 methyl group from sterol intermediates, a critical step in sterol biosynthesis. C14DM deletion in *L. major* results in a complete loss of ergostane-based sterols what is largely replaced by 14-methylated sterol intermediates. This drastic change of sterol composition leads to increased plasma membrane fluidity, extreme vulnerability to heat and significant mitochondrial abnormalities leading to accumulation of reactive oxygen species (ROS) and impairment in respiration [6,7]. In this study, we further explored the stress response defects in *c14dm*$^{-}$ mutants and investigated the potential of exploiting these defects to improve drug efficacy. First, we found *c14dm*$^{-}$ mutants to be highly sensitive to membrane perturbation agents including Triton X-100 (0.0125%) and DMSO (0.9%), as a large portion of them died within hours while WT and add-back parasites were mostly alive (Figure 1). In addition, *c14dm*$^{-}$ cells showed more pronounced volume changes than WT parasites under hypo- and hyper-osmolarity stress (Figure 2). These findings suggest that the accumulation of 14-methylated sterols, mainly 14-methylfecosterol, renders the plasma membrane more permeable and less stable.

We also tested the role of C14DM in parasite's response to *Pseudomonas aeruginosa* products. During the sandfly stage, *Leishmania* resides in the midgut which harbors a diverse and dynamic microbiota [23,37,38]. *Leishmania* interacts with sandfly midgut microbiome through competition for nutrients and space; parasites also encounter toxins and other bacterial metabolites; and the content

 doi:10.20944/preprints202508.0200.v1

and abundance of microbiome can either facilitate or hinder *Leishmania* survival and development [39–41]. During the mammalian stage, *Leishmania* and bacteria coinfections have been reported to exacerbate skin lesions [21,42]. Here we used *P. aeruginosa* as a model to evaluate the impact of sterol synthesis on *Leishmania*-bacteria interactions. As shown in Figure 3A, the spent medium from *P. aeruginosa* had potent leishmanicidal activity as ~80% of WT *L. major* promastigotes were lysed with 60 min. This is likely due to the cytotoxic substances secreted by *P. aeruginosa* including apoptosis-inducing toxins and pore-forming toxins [24,25]. Significantly, loss of C14DM led to a much more rapid cell death, indicating that the plasma membrane defects in *c14dm*$^-$ mutants enhanced the cytotoxicity of *P. aeruginosa* spent medium. *C4dm*$^-$ mutants also exhibited increased sensitivity to pyocyanin, a pigmented secondary metabolite from *P. aeruginosa* which targets the electron transport chain causing the accumulation of ROS [26,27]. It is possible that pyocyanin exacerbates the mitochondrial injury in *c14dm*$^-$ leading to rapid cell death.

Additionally, we examined whether C14DM-deletion may affect parasite's ability to carry out autophagy by monitoring the clustering (puncta formation) and lipidation of GFP-ATG8 in stationary phase culture. Autophagy is not only important for the recycling of cellular components and nutrients, but also the transition from replicating promastigotes to infective metacyclics and then intracellular amastigotes [30,43]. The autophagy defects exhibited by *c14dm*$^-$ may contribute to their compromised virulence and tolerance to starvation stress (Figure 4 and supplemental Figures S1 and S2). It is not clear how perturbation of sterol synthesis affects the autophagy process, and future studies may focus on the roles of sterols in vesicular trafficking and nutrient level sensing.

Our previous study on *c14dm*$^-$ has revealed an increased sensitivity of these mutants to pentamidine (PENT), a drug known to be sequestered into the mitochondria of *Leishmania* in a membrane potential dependent manner to exert its activity [7,34]. Here we discovered a similar hyper-susceptibility of *c14dm*$^-$ to EtBr and antimony (Sb III) (Figure 5). As a DNA-intercalating agent, EtBr impairs both kinetoplast DNA and nuclear DNA replication [33]. The targets of antimony-based drugs include the trypanothione reductase/trypanothione system, DNA topoisomerase I and host immunity, leading to elevated ROS stress, DNA replication defects and activated immune response [44–46]. The high membrane permeability in *c14dm*$^-$ may increase drug uptake and target binding in *c14dm*$^-$. Additionally, these drugs may exacerbate the existing mitochondrial and ROS stress in *c14dm*$^-$ resulting in more pronounced cell death or growth inhibition.

Like *c14dm*$^-$, *L. major* WT promastigotes grown in the presence of ITZ (a potent inhibitor of C14DM) [6] are highly susceptible to PENT [7]. Here we observed similar findings with *L. donovani* and *L. mexicana*. When used in combination, PENT and ITZ inhibited the growth of these parasites at a higher level than PENT/ITZ alone (Figure 6). By plotting the EC50 values of inhibitor combinations in an isobologram, we revealed a synergistic interaction between PENT and ITZ (instead of additive or antagonistic interactions) (Figure 6) [35]. Finally, chemical inhibition of C14DM by ITZ also caused hypersensitivity to antimony III and PENT in the axenic amastigotes of *L. mexicana*, raising the possibility that such a combination strategy may be viable in vivo (Figure 7).

In summary, we revealed new insights into the plasma membrane defects in C14DM-null mutants and the potential of using inhibitor combinations to improve the efficacy of current antileishmanial drugs. Future work will explore how lipid metabolism affects *Leishmania* development in the sandfly and the potential of synergistic drug combination in the mammalian host which could result in improved efficacy and reduced side effects.

4. Materials and Methods

4.1. Materials

Pyocyanin, potassium antimony III tartrate, ethidium bromide (EtBr), itraconazole (ITZ), and pentamidine (PENT) were purchased from Sigma-Aldrich Co (St. Louis, MO). Stock solutions for these chemicals were prepared in sterile phosphate-buffered saline (PBS) or DMSO (for ITZ and

 doi:10.20944/preprints202508.0200.v1

PENT) and stored in aliquots at –20 °C. Rabbit anti-GFP antibody was purchased from Abcam (Waltham, MA). All other reagents were purchased from Thermo Fisher Scientific unless specified.

4.2. Leishmania Culture

L. major LV39 clone 5 wild type (WT) (Rho/SU/59/P), *c14dm*$^{-}$ (*C14DM*-null mutant), and *c14dm*$^{-}$/+*C14DM* (the complemented or add-back line) promastigotes were cultivated at 27°C in complete M199 media (pH 7.4) with 10% fetal bovine serum and additional supplements as previously described [6,17]. The same medium and condition were used to culture *Leishmania donovani* strain 1S2D (MHOM/SD/62/1S-CL2D) and *Leishmania mexicana* M379 (MNYC/BZ/62/M379) promastigotes. *L. mexicana* axenic amastigotes were cultured using an amastigote medium based on the *Drosophila* Schneider's medium supplemented with 20% fetal bovine serum and 0.0015% hemin (pH 5.4) in vented flasks in a humidified 32°C/5% CO_2 incubator [36,47]. To monitor cell growth over time, culture densities were determined using a hemacytometer. Cell viability was measured by flow cytometry after staining with 0.5 μg/ml of propidium iodide using an Attune Acoustic Flow Cytometer [6].

4.3. To Determine the Effects of Membrane Perturbing agents, P. aeruginosa PA14 Conditioned Medium, Pyocyanin, and Chemical Inhibitors

To test the effect of membrane disrupting agents, *L. major* promastigotes were cultivated to 2.0 x 10^6 cells/ml in complete 1 x M199 medium and treated with Triton X-100 (final concentration: 0.0125%) or DMSO (final concentration: 0.9%). Cell viability was measured at various time points by flow cytometry after staining with propidium iodide. We titrated the concentration ranges of Triton X-100 (0–0.1%) and DMSO (0–2%) to determine the optimal concentrations that reveal the difference between WT and *c14dm*$^{-}$. *P. aeruginosa* PA14 conditioned medium was separated from PA14 bacteria grown in complete 1 x M199 medium (OD600: 2.9–3.0) by centrifugation (8000g, 10 min) followed by filtration through 0.2-micron filters. Log phase promastigotes were resuspended in the PA14 conditioned medium at 5.0 × 10^6 cells/ml and cell survival was measured by counting the number of promastigotes/ml using a hemocytometer at 0–60 minutes post exposure.

To determine sensitivity to pyocyanin, log phase promastigotes were inoculated in complete 1 x M199 medium at 2.0 × 10^5 cells/ml and challenged with pyocyanin ranging from 31.25 μM to 250 μM. After incubation at 27ºC for 24 hours, cell viability was measured by flow cytometry.

To measure sensitivity to potassium antimony III tartrate, ethidium bromide (EtBr), ITZ, or PENT, log phase promastigotes were inoculated in complete 1 x M199 medium at 2.0 × 10^5 cells/ml and exposed to various concentrations of inhibitors. Culture densities were determined using a Beckman Z2 Coulter Counter after 48 hours. The effective concentrations required to inhibit growth by 50% (EC50s) were determined using cells grown in the absence of inhibitors as controls. Similar assays were performed with *L. mexicana* axenic amastigotes cultivated in the amastigote medium.

4.4. Synergy Calculations

To determine if the effect produced by a combination of inhibitors is greater than the sum of the effects produced by each inhibitor alone, a classical isobologram was constructed by plotting EC50s of drugs that acted either singularly or in combination. Fractional inhibitory concentration (FIC) was calculated as previously described [35]:

$$FIC = EC50_{XY}/EC50_X + EC50_{YX}/EC50_Y$$

$EC50_X$ is the EC50 value for drug X (PENT) acting alone, and $EC50_{XY}$ is the EC50 of the same drug in the presence of a sub-optimal concentration of drug Y (ITZ). Similarly, $EC50_Y$ is the EC50 value for drug Y (ITZ) acting alone, and $EC50_{YX}$ is the EC50 of the same drug in the presence of a sub-optimal concentration of drug X (PENT). If the value of the FIC is $\leq$ 0.5, a synergic effect is diagnosed, for 0.5 < FIC $\leq$1 the effects are considered additive and for FIC > 1.0 the combined effects are considered antagonistic [35].

 doi:10.20944/preprints202508.0200.v1

4.5. Response to Osmotic Stress

Log phase promastigotes were collected by centrifugation (2000g, 10 min), washed twice with PBS and resuspended in the isotonic 1 x Iso-Cl buffer (20 mM HEPES pH 7.4, 11 mM glucose, 1 mM $CaCl_2$, 0.8 mM $MgSO_4$, 137 mM NaCl, 4 mM KCl, 1.5 mM K_2HPO_4, and 8.5 mM Na_2HPO_4, final osmolarity: 301 mOsmol/L) at 2×10^8 cells/ml. Cell suspensions were distributed into a 96-well plate with 150 µl per well in triplicate. To determine cells' response to osmotic changes, 150 µl of deionized water or 4 x Iso-Cl buffer was added to each well to induce hypotonic or hypertonic stress. For the isotonic control, 150 µl of 1 x Iso-Cl buffer was added. Relative cell volume changes were assessed by monitoring absorbance at 550 nm by light scattering where a decrease corresponded to an increase in cell volume [18]. Absorbance was measured every 30 sec for 60 min using a Biotek plate reader, where every time point was calculated in the automated kinetic format and orbital shaking was performed for 5 sec after each reading. Absorbance values were normalized to cells under the isotonic condition.

4.6. Autophagy Assays and Microscopy

For autophagy studies, the GFP-ATG8 open reading frame was cloned into the pXG-HYG plasmid [29,48] and introduced into *L. major* WT, *c14dm*$^{-}$ or *c14dm*$^{-}$*/+C14DM* promastigotes by electroporation. Transfectants were selected and grown in presence of 40 µg/ml of hygromycin as WT *+GFP-ATG8*, *c14dm*$^{-}$ *+GFP-ATG8* or *c14dm*$^{-}$*/+C14DM +GFP-ATG8*.

To measure the percentage of cells with autophagosomes containing GFP-ATG8, promastigotes were analyzed daily from log phase to late stationary phase by fluorescence microscopy as previously described [28,29,43] using a BX-51 epifluorescence microscope. At each measuring point, a minimum of 200 cells per group were examined and categorized as having either cytosolic or spotty, autophagosomal GFP-ATG8 localization (puncta). In addition, Western blot was performed using an anti-GFP antibody to detect both phosphatidylethanolamine (PE)-conjugated and unconjugated GFP-ATG8 [29]. Signals from Western blot were quantified using a Fuji phosphoimager.

4.7. Statistical Analysis

Experimental values in all figures were averaged from three to five independent biological repeats and error bars represented standard deviations. Differences were assessed by one-way ANOVA (for three or more groups) using the Sigmaplot 13.0 software (Systat Software Inc, San Jose, CA). *P* values indicating statistical significance were grouped in all Figures (***: $p < 0.001$, **: $p < 0.01$, *: $p < 0.05$).

Supplementary Materials: The following supporting information can be downloaded at the website of this paper posted on Preprints.org, Figure S1: *C14dm*$^{-}$*mutants* show defects in autophagy; Figure S2. Full size Western blot images for Figure 4D and Figure S1E.

Author Contributions: Conceptualization, K.Z.; methodology, K.Z., S. Moitra, and S. Mukherjee; formal analysis, K.Z., S. Moitra, and S. Mukherjee; data curation, K.Z.; writing—original draft preparation, K.Z; writing—review and editing, K.Z., S. Moitra, and S. Mukherjee; supervision, K.Z.; project administration, K.Z.; funding acquisition, K.Z. All authors have read and agreed to the published version of the manuscript.

Funding: This research was funded by National Institutes of Health grants R15AI156746 (KZ) and R01AI139198 (MW).

Institutional Review Board Statement: Not applicable.

Informed Consent Statement: Not applicable.

Data Availability Statement: The original contributions presented in the study are included in the article/supplementary material, further inquiries can be directed to the corresponding author.

Acknowledgments: The authors thank Dr. Catherine Wakeman (Texas Tech University) for the Biotek plate reader used in the light scattering measurements at 550 nm.

 doi:10.20944/preprints202508.0200.v1

Conflicts of Interest: The authors declare no conflicts of interest.

References

1. Pace, D. Leishmaniasis. *The Journal of infection* 2014, *69 Suppl 1*, S10-18. https://doi.org/10.1016/j.jinf.2014.07.016.
2. Uliana, S.R.B.; Trinconi, C.T.; Coelho, A.C. Chemotherapy of leishmaniasis: present challenges. *Parasitology* 2018, *145*, 464-480. https://doi.org/10.1017/S0031182016002523.
3. de Souza, W.; Rodrigues, J.C. Sterol Biosynthesis Pathway as Target for Anti-trypanosomatid Drugs. *Interdisciplinary perspectives on infectious diseases* 2009, *2009*, 642502. https://doi.org/10.1155/2009/642502.
4. de Macedo-Silva, S.T.; de Souza, W.; Rodrigues, J.C. Sterol Biosynthesis Pathway as an Alternative for the Anti-Protozoan Parasite Chemotherapy. *Current medicinal chemistry* 2015, *22*, 2186-2198.
5. Tanwar, S.; Kalra, S.; Bari, V.K. Insights into the role of sterol metabolism in antifungal drug resistance: a mini-review. *Frontiers in microbiology* 2024, *15*, 1409085. https://doi.org/10.3389/fmicb.2024.1409085.
6. Xu, W.; Hsu, F.F.; Baykal, E.; Huang, J.; Zhang, K. Sterol Biosynthesis Is Required for Heat Resistance but Not Extracellular Survival in Leishmania. *PLoS pathogens* 2014, *10*, e1004427. https://doi.org/10.1371/journal.ppat.1004427.
7. Mukherjee, S.; Moitra, S.; Xu, W.; Hernandez, V.; Zhang, K. Sterol 14-alpha-demethylase is vital for mitochondrial functions and stress tolerance in Leishmania major. *PLoS pathogens* 2020, *16*, e1008810. https://doi.org/10.1371/journal.ppat.1008810.
8. Karamysheva, Z.N.; Moitra, S.; Perez, A.; Mukherjee, S.; Tikhonova, E.B.; Karamyshev, A.L.; Zhang, K. Unexpected Role of Sterol Synthesis in RNA Stability and Translation in Leishmania. *Biomedicines* 2021, *9*. https://doi.org/10.3390/biomedicines9060696.
9. McCall, L.I.; El Aroussi, A.; Choi, J.Y.; Vieira, D.F.; De Muylder, G.; Johnston, J.B.; Chen, S.; Kellar, D.; Siqueira-Neto, J.L.; Roush, W.R.; et al. Targeting Ergosterol biosynthesis in Leishmania donovani: essentiality of sterol 14 alpha-demethylase. *PLoS neglected tropical diseases* 2015, *9*, e0003588. https://doi.org/10.1371/journal.pntd.0003588.
10. Tulloch, L.B.; Tinti, M.; Wall, R.J.; Weidt, S.K.; Corpas-Lopez, V.; Dey, G.; Smith, T.K.; Fairlamb, A.H.; Barrett, M.P.; Wyllie, S. Sterol 14-alpha demethylase (CYP51) activity in Leishmania donovani is likely dependent upon cytochrome P450 reductase 1. *PLoS pathogens* 2024, *20*, e1012382. https://doi.org/10.1371/journal.ppat.1012382.
11. Francesconi, V.A.; Francesconi, F.; Ramasawmy, R.; Romero, G.A.S.; Alecrim, M. Failure of fluconazole in treating cutaneous leishmaniasis caused by Leishmania guyanensis in the Brazilian Amazon: An open, nonrandomized phase 2 trial. *PLoS neglected tropical diseases* 2018, *12*, e0006225. https://doi.org/10.1371/journal.pntd.0006225.
12. Beach, D.H.; Goad, L.J.; Holz, G.G., Jr. Effects of antimycotic azoles on growth and sterol biosynthesis of Leishmania promastigotes. *Molecular and biochemical parasitology* 1988, *31*, 149-162.
13. Yamamoto, E.S.; Jesus, J.A.; Bezerra-Souza, A.; Laurenti, M.D.; Ribeiro, S.P.; Passero, L.F.D. Activity of Fenticonazole, Tioconazole and Nystatin on New World Leishmania Species. *Curr Top Med Chem* 2018, *18*, 2338-2346. https://doi.org/10.2174/1568026619666181220114627.
14. Fernandez, O.L.; Rosales-Chilama, M.; Quintero, N.; Travi, B.L.; Wetzel, D.M.; Gomez, M.A.; Saravia, N.G. Potency and Preclinical Evidence of Synergy of Oral Azole Drugs and Miltefosine in an Ex Vivo Model of Leishmania (Viannia) panamensis Infection. *Antimicrobial agents and chemotherapy* 2022, *66*, e0142521. https://doi.org/10.1128/AAC.01425-21.
15. Joice, A.C.; Yang, S.; Farahat, A.A.; Meeds, H.; Feng, M.; Li, J.; Boykin, D.W.; Wang, M.Z.; Werbovetz, K.A. Antileishmanial Efficacy and Pharmacokinetics of DB766-Azole Combinations. *Antimicrobial agents and chemotherapy* 2018, *62*. https://doi.org/10.1128/AAC.01129-17.
16. Koley, D.; Bard, A.J. Triton X-100 concentration effects on membrane permeability of a single HeLa cell by scanning electrochemical microscopy (SECM). *Proceedings of the National Academy of Sciences of the United States of America* 2010, *107*, 16783-16787. https://doi.org/10.1073/pnas.1011614107.

 doi:10.20944/preprints202508.0200.v1

17. Kapler, G.M.; Coburn, C.M.; Beverley, S.M. Stable transfection of the human parasite *Leishmania major* delineates a 30-kilobase region sufficient for extrachromosomal replication and expression. *Mol Cell Biol* 1990, *10*, 1084-1094.
18. Dagger, F.; Valdivieso, E.; Marcano, A.K.; Ayesta, C. Regulatory volume decrease in Leishmania mexicana: effect of anti-microtubule drugs. *Memorias do Instituto Oswaldo Cruz* 2013, *108*, 84-90. https://doi.org/10.1590/s0074-02762013000100014.
19. Tom, A.; Kumar, N.P.; Kumar, A.; Saini, P. Interactions between Leishmania parasite and sandfly: a review. *Parasitology research* 2023, *123*, 6. https://doi.org/10.1007/s00436-023-08043-7.
20. Campolina, T.B.; Villegas, L.E.M.; Monteiro, C.C.; Pimenta, P.F.P.; Secundino, N.F.C. Tripartite interactions: Leishmania, microbiota and Lutzomyia longipalpis. *PLoS neglected tropical diseases* 2020, *14*, e0008666. https://doi.org/10.1371/journal.pntd.0008666.
21. Borbon, T.Y.; Scorza, B.M.; Clay, G.M.; Lima Nobre de Queiroz, F.; Sariol, A.J.; Bowen, J.L.; Chen, Y.; Zhanbolat, B.; Parlet, C.P.; Valadares, D.G.; et al. Coinfection with Leishmania major and Staphylococcus aureus enhances the pathologic responses to both microbes through a pathway involving IL-17A. *PLoS neglected tropical diseases* 2019, *13*, e0007247. https://doi.org/10.1371/journal.pntd.0007247.
22. Al-Alousy, N.W.; Al-Nasiri, F.S. Bacterial infections associated with cutaneous leishmaniasis in Salah Al-Din province, Iraq. *Microb Pathog* 2025, *198*, 107144. https://doi.org/10.1016/j.micpath.2024.107144.
23. Karimian, F.; Koosha, M.; Choubdar, N.; Oshaghi, M.A. Comparative analysis of the gut microbiota of sand fly vectors of zoonotic visceral leishmaniasis (ZVL) in Iran; host-environment interplay shapes diversity. *PLoS neglected tropical diseases* 2022, *16*, e0010609. https://doi.org/10.1371/journal.pntd.0010609.
24. Wood, S.J.; Goldufsky, J.W.; Seu, M.Y.; Dorafshar, A.H.; Shafikhani, S.H. Pseudomonas aeruginosa Cytotoxins: Mechanisms of Cytotoxicity and Impact on Inflammatory Responses. *Cells* 2023, *12*. https://doi.org/10.3390/cells12010195.
25. Deng, Q.; Zhang, Y.; Barbieri, J.T. Intracellular trafficking of Pseudomonas ExoS, a type III cytotoxin. *Traffic* 2007, *8*, 1331-1345. https://doi.org/10.1111/j.1600-0854.2007.00626.x.
26. Abdelaziz, A.A.; Kamer, A.M.A.; Al-Monofy, K.B.; Al-Madboly, L.A. Pseudomonas aeruginosa's greenish-blue pigment pyocyanin: its production and biological activities. *Microb Cell Fact* 2023, *22*, 110. https://doi.org/10.1186/s12934-023-02122-1.
27. Goncalves, T.; Vasconcelos, U. Colour Me Blue: The History and the Biotechnological Potential of Pyocyanin. *Molecules (Basel, Switzerland)* 2021, *26*. https://doi.org/10.3390/molecules26040927.
28. Williams, R.A.; Smith, T.K.; Cull, B.; Mottram, J.C.; Coombs, G.H. ATG5 is essential for ATG8-dependent autophagy and mitochondrial homeostasis in Leishmania major. *PLoS pathogens* 2012, *8*, e1002695. https://doi.org/10.1371/journal.ppat.1002695.
29. Williams, R.A.; Woods, K.L.; Juliano, L.; Mottram, J.C.; Coombs, G.H. Characterization of unusual families of ATG8-like proteins and ATG12 in the protozoan parasite Leishmania major. *Autophagy* 2009, *5*, 159-172.
30. Besteiro, S.; Williams, R.A.; Morrison, L.S.; Coombs, G.H.; Mottram, J.C. Endosome sorting and autophagy are essential for differentiation and virulence of *Leishmania major*. *The Journal of biological chemistry* 2006, *281*, 11384-11396.
31. J, B.; M, B.M.; Chanda, K. An Overview on the Therapeutics of Neglected Infectious Diseases-Leishmaniasis and Chagas Diseases. *Frontiers in chemistry* 2021, *9*, 622286. https://doi.org/10.3389/fchem.2021.622286.
32. Riou, G.; Delain, E. Abnormal circular DNA molecules induced by ethidium bromide in the kinetoplast of Trypanosoma cruzi. *Proceedings of the National Academy of Sciences of the United States of America* 1969, *64*, 618-625. https://doi.org/10.1073/pnas.64.2.618.
33. Roy Chowdhury, A.; Bakshi, R.; Wang, J.; Yildirir, G.; Liu, B.; Pappas-Brown, V.; Tolun, G.; Griffith, J.D.; Shapiro, T.A.; Jensen, R.E.; et al. The killing of African trypanosomes by ethidium bromide. *PLoS pathogens* 2010, *6*, e1001226. https://doi.org/10.1371/journal.ppat.1001226.
34. Mukherjee, A.; Padmanabhan, P.K.; Sahani, M.H.; Barrett, M.P.; Madhubala, R. Roles for mitochondria in pentamidine susceptibility and resistance in Leishmania donovani. *Molecular and biochemical parasitology* 2006, *145*, 1-10. https://doi.org/10.1016/j.molbiopara.2005.08.016.

 doi:10.20944/preprints202508.0200.v1

35. Hallander, H.O.; Dornbusch, K.; Gezelius, L.; Jacobson, K.; Karlsson, I. Synergism between aminoglycosides and cephalosporins with antipseudomonal activity: interaction index and killing curve method. *Antimicrobial agents and chemotherapy* 1982, *22*, 743-752.
36. Gupta, N.; Goyal, N.; Rastogi, A.K. In vitro cultivation and characterization of axenic amastigotes of Leishmania. *Trends in parasitology* 2001, *17*, 150-153.
37. Tabbabi, A.; Mizushima, D.; Yamamoto, D.S.; Zhioua, E.; Kato, H. Comparative analysis of the microbiota of sand fly vectors of Leishmania major and L. tropica in a mixed focus of cutaneous leishmaniasis in southeast Tunisia; ecotype shapes the bacterial community structure. *PLoS neglected tropical diseases* 2024, *18*, e0012458. https://doi.org/10.1371/journal.pntd.0012458.
38. Fraihi, W.; Fares, W.; Perrin, P.; Dorkeld, F.; Sereno, D.; Barhoumi, W.; Sbissi, I.; Cherni, S.; Chelbi, I.; Durvasula, R.; et al. An integrated overview of the midgut bacterial flora composition of Phlebotomus perniciosus, a vector of zoonotic visceral leishmaniasis in the Western Mediterranean Basin. *PLoS neglected tropical diseases* 2017, *11*, e0005484. https://doi.org/10.1371/journal.pntd.0005484.
39. Cecilio, P.; Rogerio, L.A.; T, D.S.; Tang, K.; Willen, L.; Iniguez, E.; Meneses, C.; Chaves, L.F.; Zhang, Y.; Dos Santos Felix, L.; et al. Leishmania sand fly-transmission is disrupted by Delftia tsuruhatensis TC1 bacteria. *Nat Commun* 2025, *16*, 3571. https://doi.org/10.1038/s41467-025-58769-4.
40. Sant'Anna, M.R.; Diaz-Albiter, H.; Aguiar-Martins, K.; Al Salem, W.S.; Cavalcante, R.R.; Dillon, V.M.; Bates, P.A.; Genta, F.A.; Dillon, R.J. Colonisation resistance in the sand fly gut: Leishmania protects Lutzomyia longipalpis from bacterial infection. *Parasites & vectors* 2014, *7*, 329. https://doi.org/10.1186/1756-3305-7-329.
41. Kelly, P.H.; Bahr, S.M.; Serafim, T.D.; Ajami, N.J.; Petrosino, J.F.; Meneses, C.; Kirby, J.R.; Valenzuela, J.G.; Kamhawi, S.; Wilson, M.E. The Gut Microbiome of the Vector Lutzomyia longipalpis Is Essential for Survival of Leishmania infantum. *mBio* 2017, *8*. https://doi.org/10.1128/mBio.01121-16.
42. Gallo-Francisco, P.H.; Brocchi, M.; Giorgio, S. Leishmania and its relationships with bacteria. *Future microbiology* 2022, *17*, 199-218. https://doi.org/10.2217/fmb-2021-0133.
43. Giri, S.; Shaha, C. Leishmania donovani parasite requires Atg8 protein for infectivity and survival under stress. *Cell death & disease* 2019, *10*, 808. https://doi.org/10.1038/s41419-019-2038-7.
44. Haldar, A.K.; Sen, P.; Roy, S. Use of antimony in the treatment of leishmaniasis: current status and future directions. *Mol Biol Int* 2011, *2011*, 571242. https://doi.org/10.4061/2011/571242.
45. Wyllie, S.; Cunningham, M.L.; Fairlamb, A.H. Dual action of antimonial drugs on thiol redox metabolism in the human pathogen Leishmania donovani. *The Journal of biological chemistry* 2004, *279*, 39925-39932. https://doi.org/10.1074/jbc.M405635200.
46. Zhang, H.; Yan, R.; Liu, Y.; Yu, M.; He, Z.; Xiao, J.; Li, K.; Liu, G.; Ning, Q.; Li, Y. Progress in antileishmanial drugs: Mechanisms, challenges, and prospects. *PLoS neglected tropical diseases* 2025, *19*, e0012735. https://doi.org/10.1371/journal.pntd.0012735.
47. Bates, P.A. Axenic culture of Leishmania amastigotes. *Parasitology today (Personal ed* 1993, *9*, 143-146. https://doi.org/10.1016/0169-4758(93)90181-e.
48. Ha, D.S.; Schwarz, J.K.; Turco, S.J.; Beverley, S.M. Use of the green fluorescent protein as a marker in transfected Leishmania. *Molecular and biochemical parasitology* 1996, *77*, 57-64.